Geol Rundsch (1995) 84:175–186

ORIGINAL PAPER

J. M. González-Casado · C. Casquet
J. M. Martínez-Martínez · V. García-Dueñas

Retrograde evolution of quartz segregations from the Dos Picos shear zone in the Nevado-Filabride Complex (Betic chains, Spain). Evidence from fluid inclusions and quartz c-axis fabrics

Received: 12 February 1993 / Accepted: 23 June 1994

Abstract Synkinematic quartz veins are ubiquitous in the shear zone separating the Veleta unit from the Calar Alto unit in the internal part of the Betic Cordilleras. They have been studied with respect to quartz c-axis fabrics, microstructures and fluid inclusions. Veins were probably generated during syn-metamorphic stacking of the units at $P = 500-600$ MPa and $T = 400-500$ °C. Quartz displays two groups of microstructures in the shear zone: (1) older coarse-grained mosaics (CGM) resulting from exaggerated grain growth; and (2) younger fine-grained mosaics (FGM) developed at the expense of the former. The fine-grained mosaics show polygonal granoblastic and elongate mosaic microstructures in general, with ribbon microstructures often found near the boundary of the units. Fluids contained in secondary inclusions vary from high salinity brines to different types of CO_2 – brine mixtures and low density CO_2 fluids. Differences in composition and $P-T$ trapping conditions are indicated for the different types of inclusions. Some fluid inclusions are older than the FGM, whereas others are younger, thus constraining the $P-T$ conditions at which the two microstructural events took place. Fluid inclusion evidence suggests conditions of $P_{fluid} > 170$ MPa and $T \geqq 370-430$ °C for the CGM and $P_{fluid} \geqq 20-80$ MPa and $T > 340$ °C for the FGM.

The quartz c-axis fabrics dealt with here correspond to the second recrystallization event, as little evidence of older fabrics is preserved in the shear zone. C-axis patterns vary across the shear zone from slightly asymmetrical type I crossed girdles in the hanging wall and footwall to more asymmetrical crossed girdles at the boundary of the units. This indicates a correlative increase in the magnitude of the heterogeneous shear strain in the same direction. Most of the deformation is concentrated at the top of the Veleta unit. The sense of movement is top to the west, in agreement with other kinematic markers.

The quartz c-axis fabrics resulted from dynamic recrystallization during simple shear. The retrograde $P-T$ path inferred from fluid inclusion analysis, along with other geological and geochronological evidence, indicates that this deformation is coeval with a reduction in the crustal overburden.

Geochronological and stratigraphic data show that the proposed Dos Picos extensional detachment, separating the Calar Alto and Veleta units, took place during the early Miocene, synchronous with the intense thinning of the Nevado-Filábride Complex and of the whole continental crust underlying the Alborán Basin.

Key words Betic chain · Shear zones · Quartz veins · C-axis fabrics · Fluid inclusions · Extensional tectonics

J. M. González-Casado (✉)
Departamento de Q. A. Geología y Geoquímica, Universidad Autónoma, 28049 Madrid, Spain FAX 34-1-3974900

C. Casquet
Departamento de Petrología, Universidad Complutense, 28040 Madrid, Spain FAX 34-1-5442535

J. M. Martínez-Martínez · V. García-Dueñas
Departamento de Geodinámica, IAGM, CSIC-Universidad de Granada, 18071 Granada, Spain FAX 34-58-243352

Introduction

One very common feature of regionally metamorphosed rocks of pelitic composition is the occurrence of deformed quartz-rich veins and lenses. Many authors have suggested that these quartz veins are the result of tensional fluid-assisted failure of the rock during the earlier stages of synmetamorphic deformative phases (e.g. Phillips, 1972; Norris and Hendley, 1976; Etheridge, 1983, Yardley, 1986).

Quartz c-axis patterns in quartzites have proved to be very reliable in deciphering strain symmetry, shear sense and the value of strain (Lister et al., 1978; Behrmann and Platt, 1982; Jessell, 1988 a; 1988 b; Law, 1987; 1990; Law et al., 1990). Petrofabric analysis, however, has not been extensively used on deformed quartz veins, apparently because of the complex deformation/recrystallization histories undergone by these rocks.

Our study deals with the crystallographic fabric and texture of plastically deformed quartz veins and their

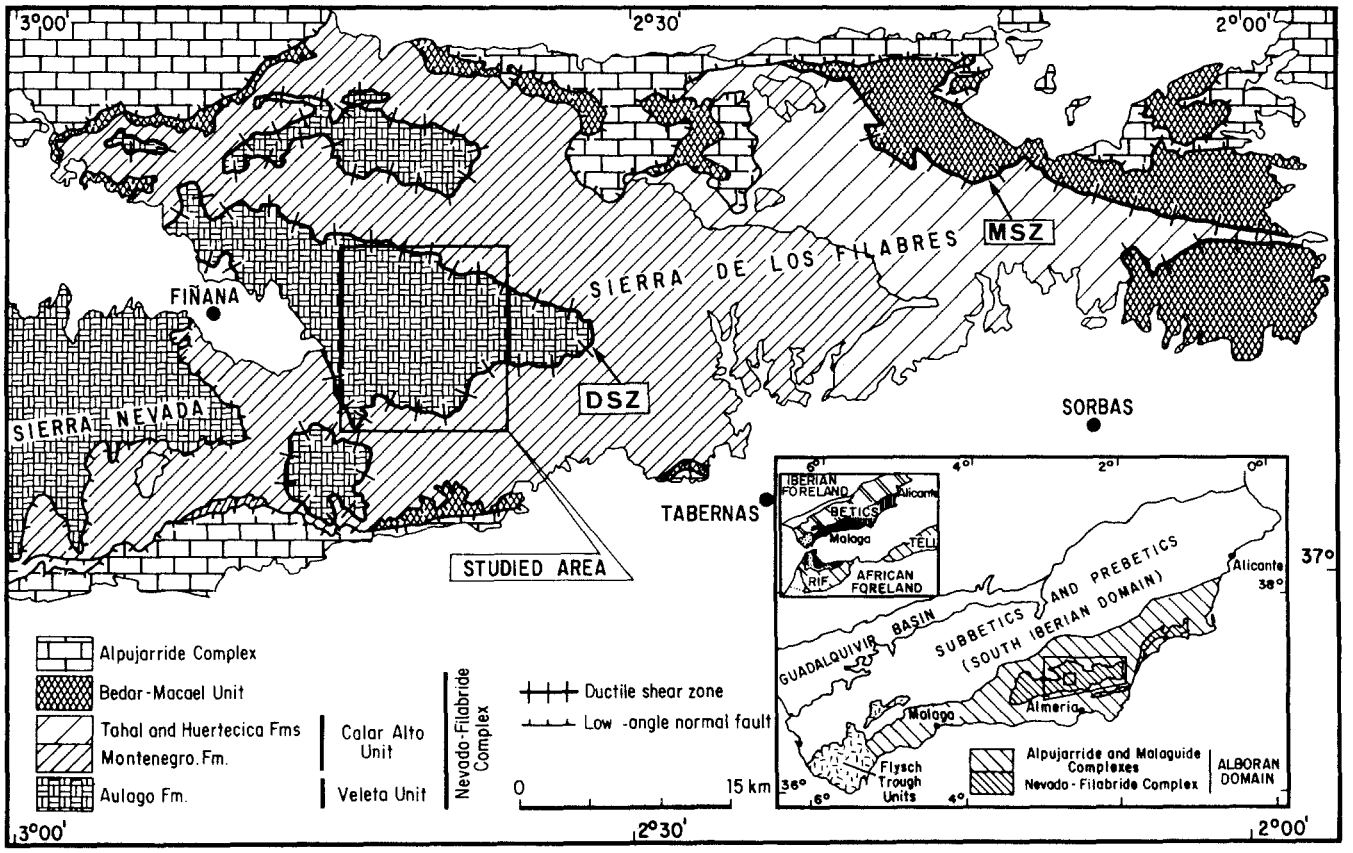

Fig. 1. The Nevado-Filabride Complex in the Sierra de Los Filabres area. DSZ = Dos Picos shear zone; MSZ = Marchal shear zone. Lithological formations and tectonic units after García-Dueñas et al. (1988)

potential use in structural research. In addition to crystallographic and microstructural work, the approach followed here includes the analysis of fluid inclusions. Trails of secondary fluid inclusions can be used as chronological markers and can be helpful in unravelling the microstructural history of the veins.

Quartz veins and lenses are ubiquitous in metapelites of the Nevado-Filábride Complex of the Alborán crustal domain (Betic chains) (Fig. 1). Samples were taken from rocks situated both outside and inside a ductile shear zone approximately 500 m thick to establish the conditions under which the quartz veins were formed, to compare the deformed and non-deformed vein fabric, and to analyse the fluid inclusions. This shear zone, known as the Dos Picos shear zone (García-Dueñas et al., 1988), contains the boundary between two major tectonic elements of the Nevado-Filábride Complex.

Regional setting

The Alborán domain, in the internal part of the Betic Orogen (Fig. 1), is a segment of thinned continental crust made up of three tectonic complexes: the Nevado-Filabride, the Alpujarride and the Malaguide, in ascending order. The tectonic complexes of the Alborán domain consist of a Palaeozoic basement and a Mesozoic cover (Permo-Triassic and younger). The Nevado-Filabride and Alpujarride lithological sequences recorded a plurifacial alpine metamorphism evolving from high pressure/low temperature facies to intermediate and low pressure facies series (Nijhuis, 1964; Vissers, 1981; Gómez-Pugnaire and Fernández-Soler, 1987; Goffe et al., 1989; Bakker et al., 1989; Tubia and Gil-Ibarguchi, 1991; Azañón et al., 1992), whereas the Malaguide complex escaped Alpine metamorphism. This metamorphism developed throughout an evolutionary history in which several episodes of crustal shortening and extension can be distinguished (García-Dueñas et al., 1992; Balanya et al., 1993). The present tectonic contacts have been interpreted as brittle extensional detachments, or low angle listric normal faults (García-Dueñas et al., 1992).

The Nevado-Filabride Complex comprises a stack of at least three tectonic units (Fig. 1) that are, from bottom to top: the Veleta unit composed of a low grade metamorphic sequence of pelites; the Calar Alto unit; and the Bedar-Macael unit (for a review of the lithological, chronostratigraphic and structural aspects of the Nevado-Filábrides, see García-Dueñas et al., 1988). The upper two units have been interpreted as recumbent folds. Both the Calar Alto and Bedar-Macael units are largely composed of low to medium grade metapelites, marbles, Permian metagranites and minor Jurassic metabasites (Hebeda et al., 1980).

The Veleta unit (Fig. 1) consists of a monotonous Palaeozoic sequence of graphite-bearing schists with abundant intercalations of psammites and some beds of graphite – marble (Aulago Formation). The sequence of the Calar Alto unit, on the other hand, is made up of different types of rocks, which are, in ascending order: (1) up to 4000 m of structural thickness of graphite-rich black schist (Montenegro Formation; Palaeozoic); (2) about 1 500 m of structural thickness of psammitic schists and quartzites with metaconglomerates in the lower part and light coloured metapelites (Tahal Formation; Permian – Triassic?); and (3) up to 150 m of calcitic and dolomitic marbles (Huertecica Formation; very probably Triassic; Nijhuis, 1964; Martínez-Martínez, 1984; 1986a). Similar rock types constitute the Bedar-Macael unit, although they are not as thick and show abundant intrusive Jurassic metabasites. Permian metagranites and orthogneisses are often associated with the Montenegro Formation.

Separating these Nevado-Filabride units are two ductile shear zones (García-Dueñas et al., 1988): the Dos Picos shear zone between the Veleta and Calar Alto units, and the Marchal shear zone between the Calar Alto and Bedar-Macael units (Fig. 1). The respective unit boundaries are generally subparallel to the lithological contacts and the regional main foliation of both the hanging wall and the footwall. In short, the tectonic boundaries show neither contraction nor extension (neutral fault geometry; Williams et al., 1989). Both shear zones have been related to post-metamorphic thrusting due to the superposition of older lithological formations on younger formations and the emplacement of medium grade metamorphic rocks above low grade metamorphic rocks (Garcia-Dueñas et al., 1988).

As will be seen in the following, the results of this study based on the analysis of fluid inclusions and the distribution of fine-grained tectonites indicates the reactivation of the Dos Picos shear zone in extensional conditions.

In the studied area (Martínez-Martínez, 1986a; 1986b), the Aulago Formation (Veleta unit) and the Montenegro Formation (Calar Alto unit) are well exposed. The tectonic contact between them is marked by the Dos Picos shear zone (about 500 m wide), which has a gentle dip and westward transport sense. The shear zone displays S – L tectonites (locally mylonites) with minor structures such as mylonitic foliation, stretching lineation (trending N80E), sheath folds and pinch and swell structures.

As shown in Fig. 1, the Dos Picos shear zone is warped around an eastward plunging anticline. A late tectonic event of late Miocene age (Weijermars et al., 1985; García-Dueñas et al., 1992) gave rise to this and other very large east – west trending folds.

Quartz veins

Quartz veins are common throughout the Dos Picos shear zone. They become even more abundant in the Montenegro schists (hanging wall of the shear zone) and are also found in the Aulago schists (footwall of the shear zone), but to a lesser extent.

The veins consists for the most part of quartz with a few scattered muscovite flakes concordant to the external foliation. Quartz veins are mostly lens-shaped (Fig. 2a), although other geometries such as folds with small interlimb angles (isoclinal and flattened folds are common) can also be found. Boudinage is a common feature. The veins always lie parallel to the schistosity plane, which is also the axial surface of the folded types. A stretching lineation with the same orientation as in the host rocks (east – west) is well displayed on the vein surfaces.

The size of the veins is very variable, from one decimetre to a few metres in length, and from a few centimetres to several decimetres in thickness. The X/Y and Y/Z ratios of the veins have been measured at several points across the shear zone. The most elongate ratios ($X/Z > 6$) are found close to the boundary of the units.

Most veins in the shear zone can be interpreted as features that developed at the beginning of the stacking phase and that were subsequently boudinaged and disrupted by progressive deformation. Therefore the veins – and the surrounding schists – probably underwent significant recrystallization previous to their deformation by the structures described in association with ductile shearing.

Microstructural analysis

Quartz displays two types of microstructure in the veins: (1) colourless coarse-grained mosaics (CGM) and (2) whitish fine-grained mosaics (FGM). When both microstructural types are present in the same vein, a zonal arrangement takes place with the vein core formed by CGM and the rim by FGM (Fig. 2b).

Coarse-grained mosaics are only found in the Montenegro schists, i.e. the hanging wall, near the boundary of the units. The mosaics consist or large grains (16 mm on average) that show interpenetration in three dimensions, sutured boundaries, strong internal deformation and included relicts of muscovite flakes arranged parallel to the external foliation. These grains were probably formed by boundary migration during a stage of exaggerated grain growth. The original quartz fabric related to the earlier formation of the veins was probably destroyed by progressive deformation and recrystallization of the veins during peak metamorphic conditions, as is common in ductile shear zones (Casquet, 1985).

Fine-grained mosaics vary widely in grain shape from granoblastic to ribbons and different types of elongate mosaics. Granoblastic polygonal microstructures have been found only in the lower unit and at a distance of more than 500 m from the boundary of the units – that is, outside the shear zone. Granoblastic microstructures with incipient grain growth by boundary migration seem to be restricted to the hanging wall of the shear zone and upwards. Ribbons and elongate mosaics are found only

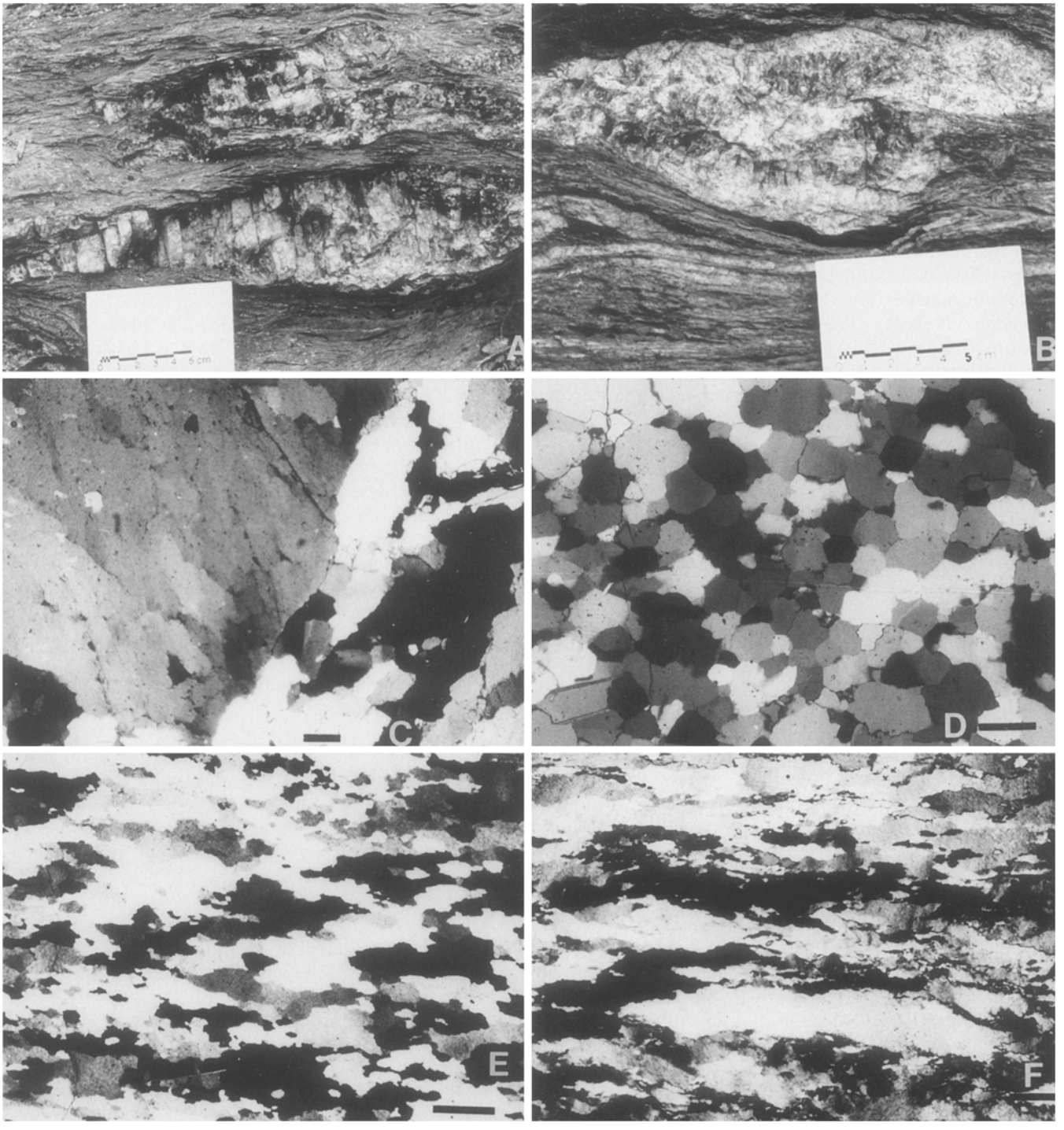

Fig. 2. **A** Lens-shaped quartz segregations in garnet-chloritoid schists from the base of the Calar Alto unit. **B** Detail of quartz lens showing a core with preserved coarse-grained mosaics (CGM), rimmed by milky quartz with a younger fine-grained mosaic texture. **C** A large quartz grain (CGM texture), with secondary fluid inclusion trails, surrounded by smaller and younger grains devoid of fluid inclusions. Sample taken in the hanging wall, close to the boundary of the units. **D** Orientated granoblastic polygonal texture from the footwall far from the boundary of the units. **E** Quartz displaying an elongate mosaic texture. **F** Quartz with a ribbon texture showing sutured boundaries and subgrains. Scale bar 1 mm. All photomicrographs (**C** to **F**) were taken under crossed polars

inside the shear zone in the proximity of the boundary of the units and most commonly in the footwall. In the lower unit, elongate mosaics occupy an intermediate position between the granoblastic microstructures and ribbons (Fig. 2d, 2e and 2f).

Both ribbons and elongate mosaics display sutured grain boundaries, with grain elongation tending towards parallelism with the external foliation. Internal substructures such as undulatory extinction and deformation bands are common.

Where CGM are preserved, fine grains form at the coarse grain boundaries, wrapping around the coarse grains. Also, the FGM develop at the contacts of the veins with the host rocks and decrease inward, giving rise to the aforementioned microstructural zoning of the veins. Coarse-grained mosaics are older than the FGM. This interpretation is also supported by the fact that CGM show abundant trails of secondary fluid inclusions, whereas they are scarce or absent in FGM. The development of FGM has therefore led to the destruction of the older grains and the fluid inclusions, suggesting that this recrystallization event is a relatively late process (Fig. 2c). This holds also true for the FGM in places where no evidence of older CGM is preserved, i.e. the footwall of the shear zone.

Fluid inclusions

Fluid inclusions are a regular feature in quartz veins. The study of fluid inclusions here is primarily intended to provide $P-T$ constraints for the retrograde $P-T$ path of the shear zone, as well as an estimate for the conditions of the recrystallization episodes undergone by the veins. Preliminary information about the composition of the fluids as well as their evolution in this part of the Alborán domain is also presented. Fluid inclusions proved to be useful as time markers for the microstructural evolution of the veins.

The study of the fluids contained in the veins was carried out using conventional microthermometric techniques on a Chaix-Meca stage, together with chemical analyses of decrepitates and crushing stages tests. Composition and densities of fluid inclusions as well as isochores were calculated from microthermometric data using the computer codes of Nicholls and Crawford (1985) and the program FLINCOR by Brown (1989) for high salinity inclusions only. Daughter crystals found in some types of fluid inclusions were checked with (SEM)-EDS techniques. Five types of fluid inclusions, all secondary, were recognized. A brief account of the microthermometric data relevant to the isochore construction follows.

1. Type I. Brine + halite inclusions (phases present, G + L + S). Salinities are high (32–35 wt.% NaCl equiv.) and $T_{\text{final homog}} = 370-430\,^{\circ}\text{C}$ (by gas disappearance). No CO_2 was detected, which implies that the XCO_2 in the fluid must be lower than 0.01 (Hedenquist and Henley, 1985).
2. Type II. $CO_2 + H_2O$ inclusions ($G + L_{CO_2} + L_{H_2O+salt}$ at 20 °C). They show large bubbles (80–100% of the total volume). CO_2 homogenizes in the liquid phase ($T_{\text{homog}} = +21$ to $+25\,^{\circ}\text{C}$). Salinities are intermediate to low. Decrepitation takes place before complete homogenization ($T_{\text{decr}} \leqq 250\,^{\circ}\text{C}$).
3. Type III. $CO_2 + H_2O$ inclusions ($G \pm L_{CO_2} + L_{H_2O+salt}$ at 20 °C). Medium to small bubbles (10–55% of the total volume). CO_2 homogenizes in the gas phase ($T_{\text{homog}} = +17$ to $+27\,^{\circ}\text{C}$). Salinities are low (3.5–7 wt.% NaCl equiv.). Homogenization takes place at 310–400 °C.
4. Type IV. CO_2-H_2O inclusions ($G + L_{H_2O+salt}$ at 20 °C). CO_2 is a very low density gas. The bubble size is 35–40% of the total volume. No homogenization temperature of the CO_2 could be determined. Salinities are intermediate (13–15 wt.% NaCl equiv.), although in some instances daughter halite crystals were found. Homogenization in the liquid phase takes place at 340–344 °C.
5. Type V. CO_2 inclusions. They consist of almost pure low density CO_2 gas [($T_{\text{melt, CO}_2} = -57.5$ to -58.1 and T_{homog} (in the gas phase) $= +1$ to $+11\,^{\circ}\text{C}$)].

The first three types of fluid inclusions are preserved only in the CGM and form correspondingly different trails, each consisting of a unique type of inclusion. The density of these trails is relatively high. Development of the FGM led to the destruction of the older large grains and of the fluid inclusions. The new grains are often clear

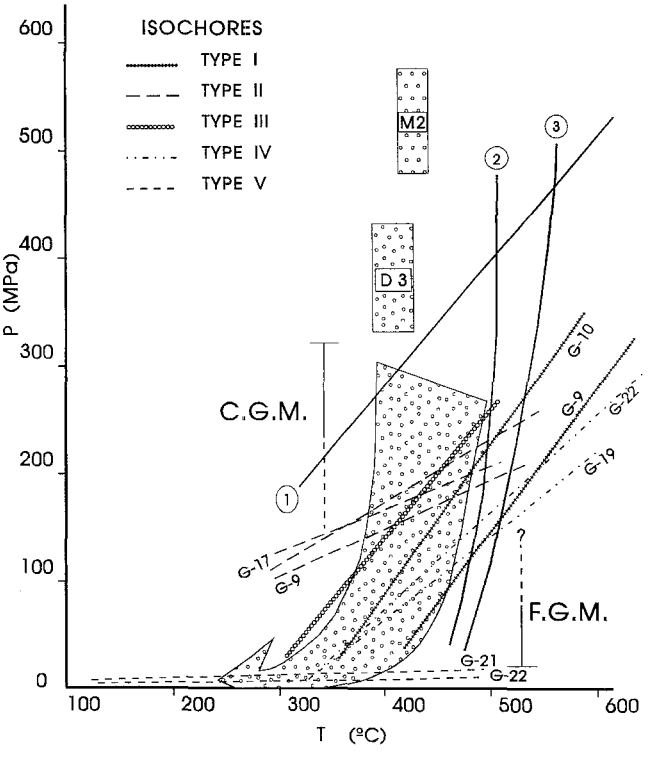

Fig. 3. $P-T$ diagram for the shear zone. Significant isochores are: type I, salt (brine) + halite; types II, III and IV, different CO_2-H_2O inclusions (see text); type V, low density CO_2. Univariant reaction curves: (1) andalusite $\rightleftharpoons$ kyanite; (2) Fe-chlorite (daphnite) + Fe-chloritoid + 2 quartz $\rightleftharpoons$ 2 almandine + 5 H_2O. (3) 48 Fe-chloritoid + 7 muscovite $\rightleftharpoons$ almandine + 6 Fe-staurolite + 7 annite + 36 H_2O. Reactions calculated with Thermocalc (Powell and Holland, 1988). M2 and D3: $P-T$ conditions during the last tectono-metamorphic event recorded in metasediments (M2 from Martínez-Martínez, 1986a; D3 from De Jong, 1991). Arrow: inferred $P-T$ path during uplift. CGM and FGM: probable conditions during development of coarse grained mosaics and fine grained mosaics respectively

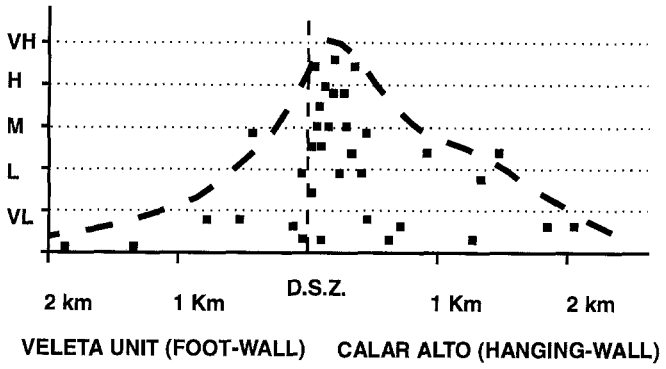

Fig. 4. Estimated content of glycerine-insoluble components in fluid inclusions across the shear zone. VL, very low; L, low; M, medium; H, high and VH, very high

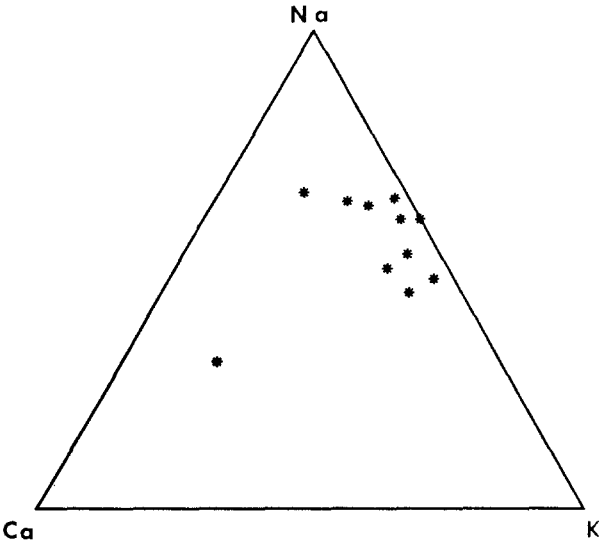

Fig. 5. Na–K–Ca relative contents in fluid inclusions from the quartz lenses obtained by chemical analyses of decrepitates

and devoid of fluid inclusions. Fluid inclusion types IV and V form scarce integranular trails in the FGM.

Coexistence in the same samples of high salinity inclusions (type I) and high CO_2–lower salinity inclusions (type II) probably reflect the immiscibility of a former homogeneous fluid (Trommsdorff and Skippen, 1988). However, the fact that each trail is formed by a unique type of inclusion suggests that after separation the fluids behaved independently and were trapped under different $P-T$ conditions.

Types IV and V probably also reflect immiscibility. In fact, they are found in the same samples, though forming different trails, and the two corresponding isochores intersect precisely at the $P-T$ homogenization values of the type IV inclusions (Fig. 3), suggesting that immiscibility probably took place at a T of approximately 340 °C and a P_{fluid} of about 15–20 MPa.

The contents of CO_2 across the shear zone, as estimated from crushing tests under glycerin, are represented in Fig. 4. The highest contents are found in the hanging wall, close to the boundary of the units, and correspond to a large extent to samples containing type II inclusions.

In all instances, cations in solution are, in order of abundance, Na, K, Ca and Mg. Figure 5 shows a plot of the decrepitates in terms of the relative contents of Na–K–Ca. High iron contents in solution are evidenced by a reddening of the surfaces on decrepitation. No clear relationship could be found between composition and distance to the boundary of the units.

P–T path constraints

Representative isochores for the different types of fluid inclusions from several veins in the shear zone are plotted in Fig. 3, along with the $P-T$ estimate for the last metamorphic event recorded in the mineral association (M 2, after Martínez-Martínez, 1986a; D 3, after De Jong, 1991). Physical conditions during the metamorphic peak in the area have been estimated at 425–450 °C and 500–600 MPa pressure (Martínez-Martínez, 1986a; see also Gómez-Pugnaire and Franz, 1988) (Fig. 3). Nevertheless, elsewhere in the Calar Alto unit an older high P/low T metamorphic event has also been recorded (Nijhuis, 1964; Martínez-Martínez, 1986a; Gómez-Pugnaire and Fernández-Soler, 1987).

Metamorphic paragenesis are similar on both sides of the tectonic boundary. The following are recorded in metapelites: quartz + muscovite + chloritoid + chlorite + garnet and quartz + muscovite + chlorite + garnet + albite. Biotite has been cited as part of these associations, but in this instance it is a biotite–chlorite intermix (Mellini et al., 1991) that was formed at a temperature lower than that of biotite itself. Kyanite pseudomorphs after Hercynian(?) andalusite have also been recorded in the Calar Alto unit (Martínez-Martínez, 1986a).

The equilibrium curves for the relevant univariant reactions (1) andalusite $\leftrightharpoons$ kyanite; and (2) Fe-chlorite (daphnite) + Fe-chloritoid + 2 quartz $\leftrightharpoons$ 2 almandine + $5H_2O$; (3) 48 Fe-chloritoid + 7 muscovite $\leftrightharpoons$ almandine + 6 Fe-staurolite + 7 annite + 36 H_2O, calculated with Thermocalc (Powell and Holland, 1988), have been included for comparison. Because of the presence of dissolved CO_2 and salts in the fluid, and the expected large departure from ideality of H_2O (in fact, immiscibility is suggested by fluid inclusions), reactions (2) and (3) probably represent upper estimates of the true temperature conditions during this last metamorphic event. The high Fe content of the minerals (Martínez-Martínez, 1986a) suggests that the effect of the Fe–Mg exchange on the equilibrium temperature is probably minor. Temperature is therefore expected to have been lower than 500 °C at pressures higher than 300 MPa. At lower pressures, fluid inclusion isochores can be used to constrain the retrograde $P-T$ path (Fig. 3).

Coarse-grained mosaics were probably formed at temperatures higher than 370–430 °C (homogenization temperatures of type I inclusions) and lower than 500 °C (see earlier arguments). As a consequence, fluid pressures had

to be higher than the value corresponding to the intersection of the isochores for inclusion Types I, II and III and the 370 isotherm. This points to fluid pressures higher than 170 MPa. The preservation of CGM in the hanging wall and close to the boundary of the units could be indicative of the existence of higher temperatures in this part of the shear zone as compared with the footwall. However, further evidence from mineral geothermometry is required to confirm this possibility.

Fine-grained mosaics must have formed at conditions between those of inclusion types I, II and III, and the $P-T$ trapping values of types IV and V, i.e. about 340 °C and 15–20 MPa for the latter. This gives a rough estimate of P_{fluid} in the range of 20 to at least 80 MPa. The low fluid pressures of trapping of type IV and V inclusions seem difficult to explain under strictly lithostatic conditions, as they would imply depths of the order of 0.5–0.7 km. Therefore, intermediate or purely hydrostatic conditions seem to have prevailed in the latest stages of uplift. If the latter is true, expected lithostatic pressures would be of the order of 40–50 MPa, or 1.5–1.9 km of depth, assuming an increase of 10 MPa fluid pressure per kilometre and an average rock density of 2700 kg/m^3.

The above considerations constrain a steep retrograde $P-T$ path, suggesting that the rate of uplift was high in this part of the Alborán domain.

Crystallographic fabrics

Crystallographic fabrics are common in plastically deformed rocks and materials. This is particularly true of minerals such as quartz and calcite which have been widely used for unravelling the kinematic history of the rocks. These fabrics can be created by means of two mechanisms: crystallographic slip (intracrystalline slip) or a combination of slip and dynamic recrystallization (for a review of this problem, see Law, 1990).

The intracrystalline slip mechanism alone has been the subject of many theoretical and experimental studies (Green et al., 1970; Hobbs et al., 1976; Nicolas and Poirer, 1976; Schmid and Casey, 1986) as well as numerous case studies. However, the role of recrystallization as an important mechanism involved in fabric development has received less attention. Jessell (1988a; 1988b) and Jessell and Lister (1990) have theoretically modelled the fabric development in mineral aggregates undergoing a combination of dynamic recrystallization and lattice rotation at different temperatures.

Microstructural evidence from our quartz veins suggests that dynamic recrystallization must have played a key part in controlling the observed quartz fabric. Consequently, a study of these veins could throw light onto the process of fabric development by dynamic recrystallization in a region such as that selected here, where temperature conditions are relatively well constrained.

Fifteen samples of almost pure quartz veins were selected out of a collection taken along three cross-sections normal to the shear zone and to the shearing direction. The structural distance of the samples with respect to the boundary of the units ranges from 2000 to 0 m. All microstructural observations and lattice orientation measurements were carried out in XZ sections parallel to the stretching lineation visible on the quartz vein surface and normal to the host rock schistosity that lies more or less subhorizontal (X axis close to a horizontal $E-W$ line; Z variable in plunge, as the shear zone is folded). About 200 c-axes were measured on each sample with the aid of a U-stage. Statistical studies of c-axis fabrics (e.g. Fernández-Rodríguez et al., 1994) show that this is the minimum number of poles to be measured to obtain a representative description of the tectonites. C-axis stereograms are represented in Fig. 6, and three types of fabrics can be distinguished:

1. In the footwall and hanging wall, far from the boundary of the units (> 1000 m), fabrics are found without preferred orientation (G1) or that bear little resemblance to samples from inside the shear zone (G22). This strongly suggests that these fabrics are older; otherwise, similar misorientated patterns should be expected inside the shear zone.
2. Fine-grained mosaics display fabric patterns that consist of two girdles with different degrees of external and internal symmetry by reference to the components of the finite strain ellipsoid (foliation and lineation; see Law, 1990). With the help of the fabric skeletons (Fig. 7), two types of c-axis patterns can be distinguished: (a) fairly symmetrical to slightly asymmetrical crossed girdles with type I (Lister, 1977) geometry (samples G10, G2, and to a lesser extent G9, G21 and G8); and (b) less symmetrical type I patterns exemplified by the successions G13, G19, G11 in the south, and G18, G14, G15 in the north. In these latter instances, one of the two girdles may almost disappear, merging into a nearly monoclinic single girdle (G19 and G15). Moreover, the external branches of the main girdle tend to turn clockwise as seen by comparing samples G18 and G15, and G19 and G13. This is consistent with a top to the west sense of movement of the shear zone.

The fabric related to the CGM could not be determined because of the large grain size and/or poor preservation in zones with FGM development.

It is interesting to note that asymmetrical fabrics are mainly found in the footwall of the Dos Picos shear zone, close to the top of the Veleta unit, whereas symmetrical fabrics occur at the bottom of the Calar Alto unit, especially at a distance of 100–300 m from the boundary of the two units. Outside the shear zone the fabrics show no preferred orientation (Figs 6 and 7).

Interpretation of the fabric patterns

The observed fabric patterns of FGM display an evolution towards the boundary of the units fairly similar to that described by Schmid and Casey for simple shear

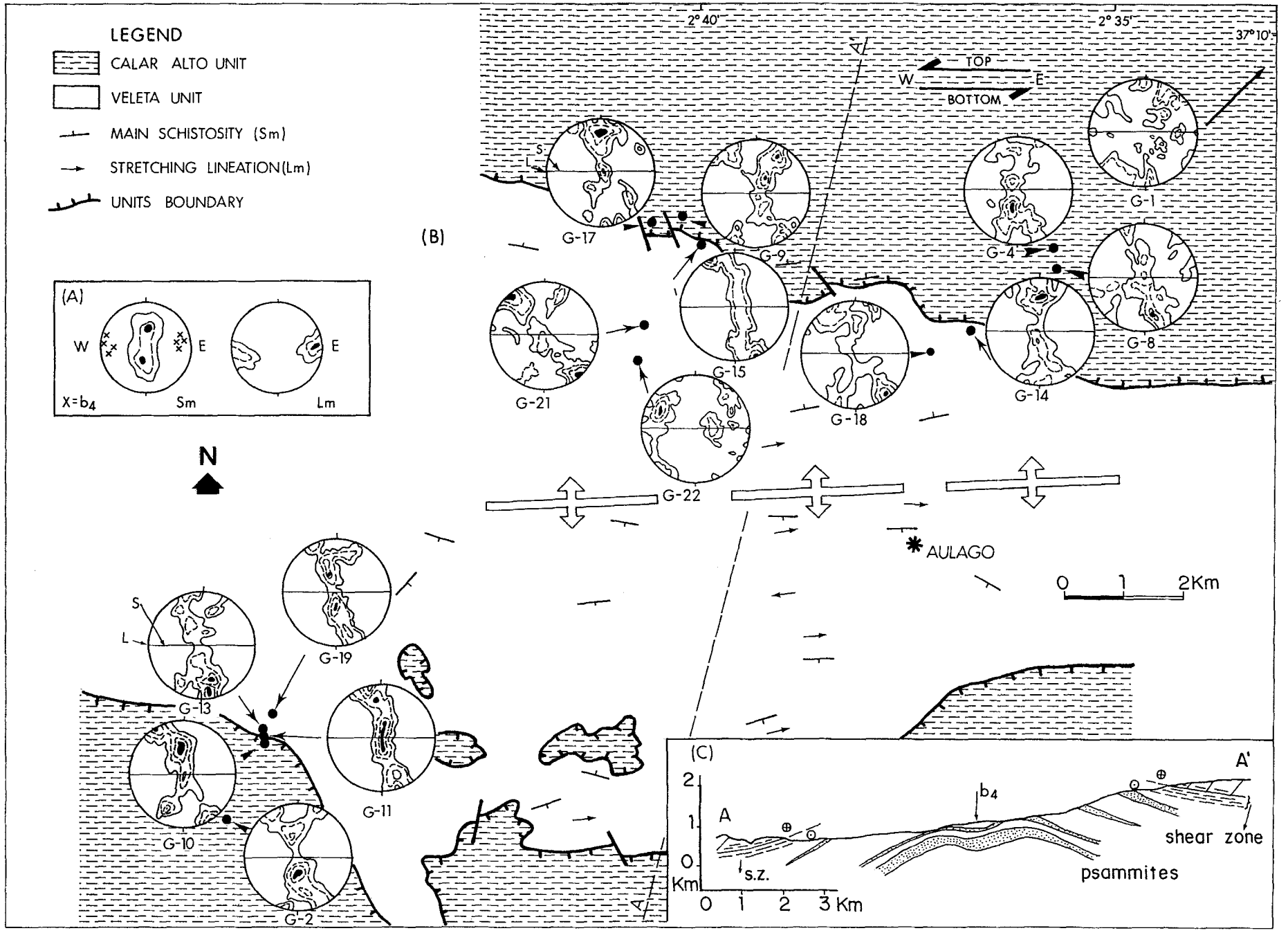
LEGEND
CALAR ALTO UNIT
VELETA UNIT
MAIN SCHISTOSITY (Sm)
STRETCHING LINEATION(Lm)
UNITS BOUNDARY
(A)
W
E
E
X=b4
Sm
Lm
N
(B)
2° 40'
2° 35'
37°10'
TOP
W
E
BOTTOM
A
A'
S
L
G-17
G-9
G-15
G-21
G-22
G-18
G-4
G-1
G-8
G-14
G-19
G-13
G-11
G-10
G-2
AULAGO
0 1 2Km
(C)
A
A'
b4
s.z.
shear zone
psammites
2
1
0
Km
0 1 2 3 Km

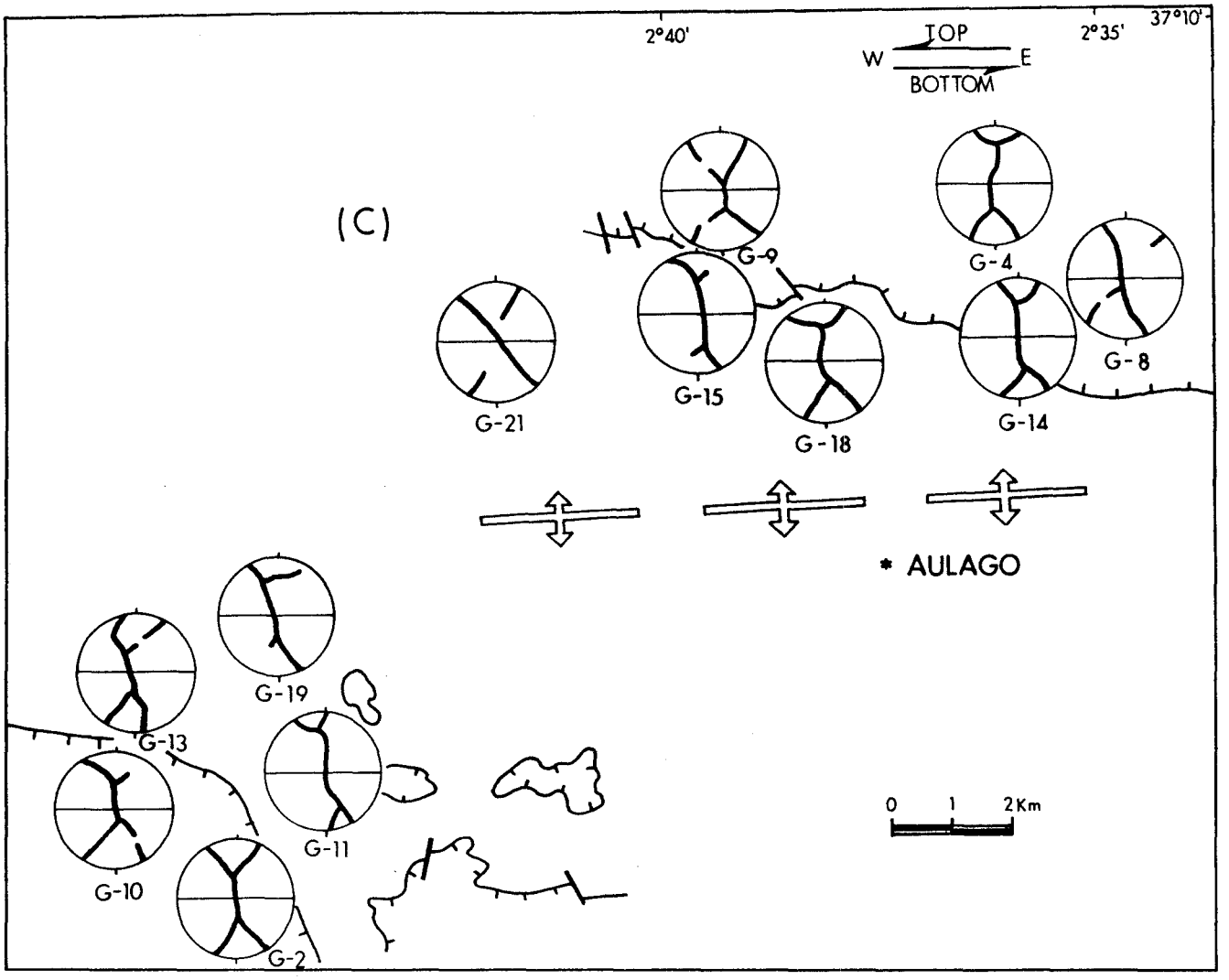

Fig. 7. Skeletons of quartz c-axis stereograms

(1986; Fig. 14). Fine-grained mosaic fabrics inside the Dos Picos shear zone evolve from close to symmetrical cross-girdles to single girdles at the boundary of the units. This suggests that the main variable controlling the fabric is probably the magnitude of the heterogeneous shear strain (see also García-Celma, 1983). This possibility is reinforced by the elongation ratios measured in the quartz veins (see earlier) that increase, on average, towards the unit boundary. The importance of shear strain seems to have been greater at the top of the Veleta unit, suggesting that most of the deformation was, in fact, concentrated in the footwall of the shear zone and in proximity to the boundary of the units.

The importance of dynamic recrystallization in the fabric evolution across the shear zone is also well displayed here. Fine-grained mosaics are developed at the expense of an older coarse-grained fabric (exaggerated grain growth texture). The inherited component of the fabric is therefore probably minor, as suggested by the regularities shown by the lattice preferred orientation patterns of FGM inside the shear zone. The fact that most of the measured grains are new and display lattice preferred orientation patterns suggests that the formation of the FGM took place syn-tectonically at the expenses of the CGM, i.e. dynamic recrystallization. Fine-grained mosaics probably evolved in a manner similar to that described by White (1973). The new crystals were formerly subgrains that by continued recovery became individual and were subsequently rotated by assisted stress-induced boundary migration. The latter is evidenced by the higly serrated grain boundaries, particularly well

Fig. 6. Simplified geological map of the area of interest. **A** Stereograms of macroscopic foliation (Sm) and stretching lineation (Lm). Both structures are folded by a late upright fold (B_4). Contours: 2, 3 and 5% per 1% of area. **B** Tectonic sketch of the area and quartz C-axis stereograms. Lower hemisphere, equal-area plots. Contours: > 5, 4, 3 and < 1%. The reference frame is defined by the foliation Sm and stretching lineation Lm. Broken lines, Calar Alto unit. **C** Geological cross-section transverse to kinematic vectors (cross inside circle, movement onto the page, point inside circle, movement of the page). Oblique ruling, Calar Alto unit

displayed in the elongate mosaics and ribbons. The process led to the removal of grains in unfavourable orientations and to the development of the final c-axis fabric. An evolution from cross-girdle to single-girdle c-axis fabric is also predicted by the model of Jessell (1988), involving a combination of lattice rotation and grain boundary migration (dynamic recrystallization). In this model the starting material is a quartz aggregate with random c-axis orientations. The quartz veins differ in that the starting material is coarse-grained quartz. The evolution here implies a first stage of syn-tectonic formation of new grains, probably with orientations controlled by the parent grains, followed by a second stage similar to that modelled by Jessell. The inherited component of the fabric was probably lost during this second stage.

The meaning of the observed distribution of c-axis maxima across the shear zone is more difficult to explain. Usually the main maxima are located at 'rhombic' and 'basal' positions, but in some diagrams (G11; Fig. 6) a maximum is found coinciding with the *Y*-axis of the finite strain ellipsoid or close to it.

Similar quartz c-axis patterns have been found in quartzites in this same shear zone by Martínez-Martínez (1986b) and other shear zones in the Alborán domain (e.g. Platt and Behrmann, 1986; Galindo-Zaldívar, 1993; Jabaloy, 1993; Jabaloy et al., 1993). Platt and Behrmann (1986) interpret the coexistence of discrete maxima at different positions as a result of uneven c-axis distribution before the main phase deformation. This possibility cannot be checked for FGM developed at the expense of CGM in the hanging wall because of the grain size of the latter. In the footwall, no evidence for inherited *Y*-maxima has been found in the outermost sample studied here (G22; Fig. 6). Martínez-Martínez (1986b) and Jabaloy et al. (1993) also recognize fabrics with *Y*-maxima close to the boundary of the units, inside the shear zone. In terms of the classic interpretation (Bouchez, 1977; Bouchez and Pecher, 1981; Lister and Dornsiepen, 1982), a prismatic ⟨a⟩ slip mechanism should be involved in the development of the *Y*-maxima. This mechanism seems to be active at moderate to high temperatures (e.g. Jessell and Lister, 1990). At very high temperatures (probably above 650–750 °C ; see Mainprice et al., 1986) prismatic ⟨c⟩ slip becomes active, leading to the development of *X*-maxima. Temperatures in this instance are moderate (less than 500 °C) and evidence of significant differences across the shear zone is still lacking. Therefore, in the absence of other evidence, we suggest that the fabric evolution displayed by FGM across the shear zone largely resulted from dynamic recrystallization of the CGM under a shear gradient at moderate temperatures. Other factors such as the strain rate or fluids (Blacic, 1975) could have also played a part in developing *Y*-maxima.

The observed fabric skeleton evolution across the Dos Picos shear zone is also similar to that found by Law et al. (1984) and Platt and Behrmann (1986). The increased asymmetry of the fabrics towards the boundary of the units is interpreted to indicate an increasing non-coaxiality of the deformation in the same sense.

The movement sense of the Dos Picos shear zone during the development of FGM, as inferred from the asymmetry of the c-axis patterns in the quartz veins, is top to the west. This agrees with the shear sense deduced in nearby quartzites and with other microstructural and structural kinematic markers (García-Dueñas et al., 1988).

The fact that the FGM fabrics were developed during the uplift of the zone along a steep $P-T$ path strongly suggests that the Dos Picos shear zone underwent a reactivation as an extensional detachment. In fact, this type of $P-T-t$ path is predicted by models involving crustal extension and not only erosion (Thompsom and Ridley, 1987).

Conclusions

The microstructural evolution of the vein quartz can be summarized as follows: an earlier stage of syn-metamorphic deformation, leading to vein formation, of which no crystallographic fabric has been recognized, was followed by a stage of exaggerated grain growth that gave rise to the CGM, most likely under static conditions and with T values close to the metamorphic peak. This stage was followed by several microfracturing episodes under quickly decreasing pressures, giving rise to the older set of fluid inclusions recorded in the CGM. Finally, a new recrystallization event producing the FGM took place during the shear zone reactivation under extensional conditions at relatively shallow depths. Dynamic recrystallization was probably an important process leading to the observed lattice orientation patterns across the shear zone.

The Dos Picos shear zone was formerly developed during a contractional event (thrusting) (García-Dueñas et al., 1988). Later on, this shear zone was reactivated under extensional conditions as many of the thrust contacts in the Alborán domain (Platt and Vissers, 1989). The FGM developed during this extensional reactivation of the shear zone under moderate temperatures ($500\,°C > T > 340\,°C$) accompanying a fast regional uplift. This is not at odds with views by García-Dueñas et al. (1992), who consider the shear zone to be the result of an early Miocene extensional event. The retrograde $P-T$ paths inferred from fluid inclusions and mineral equilibria considerations (see also Bakker et al., 1989), the occurrence of early Miocene transgressive deposits unconformably lying on rocks of the Alborán domain with peak metamorphic ages of 21 ± 2 Ma (Zeck et al., 1989), i.e. almost the same age as the sediments, evidence severe crustal thinning, consistent with the proposed extensional character of the Dos Picos shear zone. The age of the ductile shearing in other areas of the Sierra de Los Filabres is approximately 16–17 Ma (data from Monie et al., 1991). The extensional evolution discussed here is thus considered as representative of the rifting processes that led to the formation of the Alborán Sea and the South Balearic Basin in the Western Mediterranean.

Acknowledgements This work was financed by a CICYT (Spain) research grant (PB87-0461-01 and PB91-0156-01). We thank Dr C. Fernández-Rodríguez for his suggestions about fabric analysis and J. Sanders for revision of the English version. The final version has greatly benefited from suggestions by Dr R. D. Law, Dr J. H. Behrmann and an anonymous reviewer.

References

Azañón JM, García-Dueñas V, Goffe B (1992) High pressure mineral assemblages in the Trevenque unit (Central Alpujarrides, Andalucia). Geogaceta 11: 81–84

Bakker HE, De Jong K, Helmers H, Biermann C (1989) The geodynamic evolution of the Internal Zone of the Betic Cordilleras (south-east Spain): a model based on structural analysis and geothermobarometry. J Metamorphic Geol 7: 359–381

Balanya JC, Azañón JM, Sánchez-Gómez M, García-Dueñas V (1993) Pervasive ductile extension, isothermal decompression and thinning of the Jubrique unit at the Paleogene times (Alpujárride complex, Western Betics). C R Acad Sci Paris 316: 1595–1601

Behrmann JH, Platt JP (1982) Sense of nappe emplacement from quartz c-axis fabrics; an example from the Betic Cordilleras (Spain). Earth Planet Sci Lett 59: 208–215

Blasic JD (1975) Plastic-deformation mechanisms in quartz: the effect of water. Tectonophysics 27: 271–294

Bouchez JL (1977) Plastic deformation of quartzites at low temperature in an area of natural strain gradient. Tectonophysics 39: 25–50

Bouchez JL, Pecher A (1981) The Himalayan main central thrust pile and its quartz-rich tectonites in central Nepal. Tectonophysics 78: 23–50

Brown PE (1989) FLINCOR: a microcomputer program for the reduction and investigation of fluid-inclusion data. Am Mineral 74: 1390–1393

Casquet C (1985) C-O-H-N fluids in quartz segregations from a major shear zone: the Berzosa fault, Spanish Central System. J Metamorphic Geol 4: 117–130

De Jong K (1991) Tectono-metamorphic studies and radiometric dating in the Betic Cordilleras (SE Spain). PhD Thesis, Vrije Universiteit Amsterdam, 204 pp

Etherigde MA (1983) Differential stress magnitudes during regional deformation and metamorphism: upper bound imposed by tensile fracturing. Geology 11: 231–234

Fernández-Rodríguez C, González-Casado JM, Tejero R (1994) The external asymmetry of quartz c-axis fabrics: a linear approximation to its statistical description. J Struct Geol 16-2: 263–276

Galindo-Zaldívar J (1993) Geometría de las deformaciones Neógenas en Sierra Nevada (Cordilleras Béticas). Univ. Granada Ser Publ., 249 pp

García-Celma A (1983) C-axis and shape fabrics in quartz mylonites of Cap de Creus (Spain); their properties and development. PhD Thesis, Institute of Earth Sciences, Univ Utrecht, 130 pp

García-Dueñas V, Martínez-Martínez JM, Orozco M, Soto JI (1988) Plis-nappes, cisaillaments syn- à post-métamorphiques et cisaillements ductiles-fragiles en distension dans les Nevado-Filabrides (Cordillères Bétiques, Espagne). CR Acad Sci Paris 307: 1389–1395

García-Dueñas V, Balanya JC, Martínez-Martínez JM (1992) Miocene extensional detachments in the outcropping basement of the northern Alborán Basin (Betics) and their tectonic implications. Geo-Mar Lett 12: 88–95

Goffe B, Michard A, García-Dueñas V, Ganzález-Lodeiro F, Monie P, Campos J, Galindo-Zaldívar J, Jabaloy A, Martínez-Martínez JM, Simancas JF (1989) First evidence of high-pressure, low-temperature metamorphism in the Alpujárride nappes, Betic Cordilleras (SE Spain). Eur J Mineral 1: 139–142

Gómez-Pugnaire MT, Fernández-Soler JM (1987) High pressure metamorphism in metabasites from the Betic Cordilleras (SE Spain) and its evolution during the Alpine orogeny. Contrib Mineral Petrol 95: 231–244

Gómez-Pugnaire MT, Franz G (1988) Metamorphic evolution of the Palaeozoic series of the Betic Cordilleras (Nevado-Filabre complex, SE Spain) and its relationship with the alpine orogeny. Geol Rundsch 77: 619–640

Green HW, Griggs DT, Christie JM (1970) Syntectonic recrystallisation and annealing of quartz aggregates. In: Paulitsch (ed) Experimental and Natural Rock Deformation. Springer Verlag, Berlin, pp 273–335

Hebeda EH, Boelrijk NA, Priem HNA, Verdurmen EA, Verschure RH, Simon OJ (1980) Excess radiogenic Ar and undisturbed Rb–Sr systems in basic intrusives subjected to alpine metamorphism in southeastern Spain. Earth Planet Sci Lett 47: 81–90

Hedenquist JW, Henley RW (1985) The importance of CO_2 freezing point measurement of fluid inclusions: evidence from active geothermal systems and implications for epithermal ore deposition. Econ Geol 80: 1379–1406

Hobbs BE, Means WD, Williams PF (1976) An Outline of Structural Geology. Wiley, New York, 517 pp

Jabaloy A (1993) La estructura de la región occidental de la Sierra de los Filabres (Cordilleras Béticas). Univ Granada Ser Publ, 197 pp

Jabaloy A, Galindo-Zaldívar J, González-Lodeiro F (1993) The Alpujarride-Nevado-Filábride extensional shear zone, Betic Cordillera, SE Spain. J Struct Geol 15: 555–569

Jessell MW (1988 a) Simulation of fabric development in recrystallizing aggregates–I. Description of the model. J Struct Geol 10–8: 771–778

Jessell MW (1988 b) Simulation of fabric development in recrystallizing aggregates–II. Example model runs. J Struct Geol 10–8: 779–793

Jessell MW, Lister GS (1990) A simulation of the temperature dependence of quartz fabrics. In: Knipe RJ, Rutter EH (eds) Deformation Mechanisms, Rheology and Tectonics. Spec Publ Geol Soc London 54: 353–362

Law RD (1987) Heterogeneous deformation and quartz crystallographic fabric transitions: natural examples from the Moine Thrust zone at the Stack of Glencoul, northern Assynt. J Struct Geol 9: 819–833

Law RD (1990) Crystallographic fabrics: a selective review of their applications to research in structural geology. In: Knipe RJ, Rutter EH (eds) Deformation Mechanisms, Rheology and Tectonics. Spec Publ Geol Soc London 54: 335–352

Law RD, Knipe RJ, Dayan H (1984) Strain path partitioning within thrust sheet: microstructural and petrofabric evidence from the Moine thrust zone at Loch Eriboll, North-West Scotland. J Struct geol. 6: 477–497

Law RD, Schmid, SM, Wheeler J (1990) Simple shear deformation and quartz crystallographic fabrics: a possible natural example from the Torridon area of NW Scotland. J Struct Geol 12: 29–45

Lister GS (1977) Discussion: Crossed girdle c-axis fabrics in quartzites plastically deformed by plane strain and progressive simple shear. Tectonophysics 39: 51–54

Lister GS, Dornsiepen UF (1982) Fabric transitions in the Saxony granulite Terrain. J Struct Geol 4: 81–92

Lister GS, Paterson MS, Hobbs BE (1978) The simulation of fabric development in plastic deformation and its application to quartzite: the model. Tectonophysics 45: 107–158

Mainprice D, Bouchez JL, Blumenfeld P, Tubia JM (1986) Dominant *c* slip in naturally deformed quartz: implications for dramatic plastic softening at high temperature. Geology 14: 819–822

Martínez-Martínez JM (1984) Las sucesiones Nevado-Filabrides en la Sierra de los Filabres y Sierra Vevada. Correlaciones. Cuad Geol Univ Granada 12: 127–144

Martínez-Martínez JM (1986 a) Evolución tectono-metamórfica del Complejo Nevado-Filábride en el sector de unión entre Sierra Nevada y Sierra de Los Filabres (Cordilleras Béticas). Cuad Geol Univ Granada 13: 1–194

Martínez-Martínez JM (1986b) Fábricas y texturas miloníticas. Cinemática de las traslaciones en el complejo Nevado-Filábride (Cordilleras Béticas, España). Est Geol 42: 291–300

Mellini M, Nieto F, Alvarez F, Gómez-Pugnaire MT (1991) Mica-chlorite intermixing and altered chlorite from the Nevado-Filabride micaschists, Southern Spain. Eur J Mineral 3: 27–38

Monie P, Galindo-Zaldívar J, González-Lodeiro, F, Goffe B, Jabaloy A (1991) $^{40}Ar/^{39}Ar$ geochronology of Alpine tectonism in the Betic Cordilleras (southern Spain). J Geol Soc London 148: 289–297

Nicholls J, Crawford ML (1985) Fortran programs for calculation of fluid properties from microthermometric data on fluid inclusions. Comput Geosc 11: 619–645

Nicolas A, Poirer JP (1976) Crystalline Plasticity and Solid State Flow in Metamorphic Rocks. Wiley, London, 444 pp

Nijhuis HJ (1964) Plurifacial alpine metamorphism in the south-eastern Sierra de los Filábres, south of Lubrin, SE Spain. PhD Thesis, Univ Amsterdam, 151 pp

Norris RJ, Hendley RW (1976) Dewatering of a metamorphic pile. Geology 4: 333–336

Phillips WJ (1972) Hydraulic fracturing and mineralization. J Geol Soc London 128: 337–359

Platt JP, Behrmann JH (1986) Structures and fabrics in a crustal-scale shear zone, Betic Cordillera, SE Spain. J Struct Geol 8: 15–33

Platt JP, Vissers RLM (1989) Extensional collapse of thickened continental lithosphere: A working hypothesis for the Alborán Sea and Gibraltar arc. Geology 17: 540–543

Powell R, Holland TJB (1988) An internally consistent thermodynamic data set with uncertainties and correlations: 3. Applications to geobarometry, worked examples and a computer program. J Metamorphic Geol 6: 173–204

Schmid SM, Casey M (1986) Complete fabrics analysis of some commonly observed quartz C-axis patterns. In: Hobbs BE, Heard HC (eds) Mineral and Rock Deformation: Laboratory Studies – The Paterson Volume. Am. Geophys Union Geophys Monogr 36: 263–286

Thompson AB, Ridley JR (1987) Pressure–Temperature–time (P–T–t) histories of orogenic belts. Phil Trans R Soc London A 321: 27–45

Trommsdorff V, Skippen G (1988) Brines and metasomatism. Rend Soc Ital Mineral Petrol 43: 15–24

Tubia JM, Gil-Ibarguchi JI (1991) Eclogites of the Ojen nappe: a record of subduction in the Alpujarride complex (Betic Cordilleras, southern Spain). J Geol Soc London 148: 801–804

Vissers RLM (1981) A structural study of the central Sierra de los Filabres (Betic Zone, SE Spain), with emphasis on deformational processes and their relation to the alpine metamorphism. Geophys. Union Am Geol Ser 1–15: 154 pp

Weijermars R, Roep TH, Van Den Eeckhout B, Postma G, Kleverlaan K (1985) Uplift history of a Betic fold nappe inferred from Neogene–Quaternary sedimentation and tectonics (in the Sierra Alhamilla and Almeria, Sorbas and Tabernas Basins of the Betic Cordilleras, SE Spain). Geol Mijnb 64: 397–411

White S (1973) Syntectonic Recrystallization and texture development in quartz. Nature 244: 276–278

Williams GD, Powell CM, Cooper MA (1989) Geometry and kinematics of inversion tectonics. In: Cooper MA, Williams GD (eds) Inversion Tectonics. Spec Publ Geol Soc London 44: 3–15

Yardley BWD (1986) Fluid Migration and veining in the Connemara Schist, Ireland. In: Walther JW, Wood BJ (eds) Advances in Physical Geochemistry 5. Springer-Verlag, New York, pp 109–131

Zeck HP, Albat F, Hansen BT, Torres-Roldán RL, García-Casco A, Martin-Algarra A (1989) A 21 ± 2 Ma age for the termination of the ductile Alpine deformation in the internal zone of the Betic Cordilleras, South Spain. Tectonophysics 169: 215–220